FILE COPY

AD-A226 637

PAGE

Form Approved
OMB No. 0704-0188

1. Agency Use Only *(Leave blank).*	2. Report Date.	3. Report Type and Dates Covered.
	1990	Proceedings

4. Title and Subtitle.
Time-domain solution of higher-order parabolic equations

5. Funding Numbers.
Program Element No. 61153N
Project No. 3202
Task No. 0H0
Accession No. DN257015

6. Author(s).
Michael D. Collins

7. Performing Organization Name(s) and Address(es).
Naval Oceanographic and Atmospheric Research Laboratory*
Stennis Space Center, MS 39529-5004

8. Performing Organization Report Number.
PR 89:026:221

9. Sponsoring/Monitoring Agency Name(s) and Address(es).
Naval Oceanographic and Atmospheric Research Laboratory*
Stennis Space Center, MS 39529-5004

10. Sponsoring/Monitoring Agency Report Number.
PR 89:026:221

11. Supplementary Notes.
*Formerly Naval Ocean Research and Development Activity

12a. Distribution/Availability Statement.
Approved for public release; distribution is unlimited.

12b. Distribution Code.

13. Abstract *(Maximum 200 words).*

A higher-order time-domain parabolic equation (TDPE) is derived from a Pade series [7] solved numerically, and applied to underwater acoustics problems. The higher-order TDPE solution is accurate for problems involving very wide propagation angles and large variations in sound speed. Its applications include propagation near the source, propagation out to very long ranges, and propagation over a hard ocean bottom. The higher-order TDPE is valid in both shallow and deep water. The accuracy of the model is demonstrated with benchmark calculations. The model is applied to illustrate mode cutoff in a range-dependent ocean.

Keywords: (U) Transients; (U) Distributed Sensors; (U) Coherence; (U) Detection; (U) Classification (KR)

14. Subject Terms.	15. Number of Pages.
(U) Transients; (U) Distributed Sensors; (U) Coherence; (U) Detection; (U) Classification	13
	16. Price Code.

17. Security Classification of Report.	18. Security Classification of This Page.	19. Security Classification of Abstract.	20. Limitation of Abstract.
Unclassified	Unclassified	Unclassified	SAR

NSN 7540-01-280-5500

Standard Form 298 (Rev. 2-89)
Prescribed by ANSI Std. Z39-18
298-102

90 09 17 120

COMPUTATIONAL ACOUSTICS - Volume 3
D. Lee, A. Cakmak, R. Vichnevetsky (Editors)
Elsevier Science Publishers B.V. (North-Holland)
IMACS, 1990

Time-domain solution of higher-order parabolic equations

Michael D. Collins
Naval Ocean Research and Development Activity
Stennis Space Center, MS 39529

Abstract

A higher-order time-domain parabolic equation (TDPE) is derived from a Padé series[7], solved numerically, and applied to underwater acoustics problems. The higher-order TDPE solution is accurate for problems involving very wide propagation angles and large variations in sound speed. Its applications include propagation near the source, propagation out to very long ranges, and propagation over a hard ocean bottom. The higher-order TDPE is valid in both shallow and deep water. The accuracy of the model is demonstrated with benchmark calculations. The model is applied to illustrate mode cutoff in a range-dependent ocean.

1. Introduction

The parabolic equation (PE)[1] is a very useful model for range-dependent propagation calculations in underwater acoustics. The PE was originally accurate only for problems involving limited bottom interaction and narrow propagation angles. However, the PE was later extended to handle wide-angle propagation [2-4] and bottom interaction [3-5]. Benchmark comparisons showed that the wide-angle PE is accurate for many underwater acoustics problems [6]. The accuracy of the PE has recently been further improved. A higher-order PE based on a Padé series [7,8] produces solutions as accurate as the outgoing coupled mode solution[9] for very wide propagation angles and large differences in sound speed. In particular, the higher-order PE is accurate for propagation very near the source, propagation out to very long ranges, and propagation over high-speed ocean bottoms.

Two approaches exist for applying the parabolic approximation to pulse propagation. The PE has been applied to solve time-domain problems in the frequency domain using Fourier synthesis. [10,11] This is probably not an optimal approach if the solution is desired at many points in the domain. If a sequence of snapshots of the solution were desired, for example, one would have to perform Fourier synthesis at each point in each snapshot. The time-domain parabolic equation (TDPE), which is the inverse Fourier transform of the PE, has been developed for range-dependent time-domain propagation calculations.[12-16] With this approach, one automatically obtains the solution at all points in the domain.

In this paper, a higher-order TDPE is derived, solved numerically, and applied to underwater acoustic pulse propagation. In addition to allowing one to avoid Fourier synthesis, the higher-order TDPE has all of the advantages of the higher-order PE. The numerical solution is based on Galerkin's method because the depth operators are relatively complicated. The higher-order TDPE, which is accurate for propagation in both shallow and deep water, is compared with a wide-angle TDPE designed for shallow water. The accuracy of the higher-order TDPE is demonstrated

with benchmark comparisons. The model is used to illustrate mode cutoff in an ocean with an upward sloping bottom.

2. Factoring the wave equation

We work in cylindrical coordinates with r being the range from a point source and z being the depth below the ocean surface. We assume for now that the domain is stratified and that azimuth dependence can be neglected. We remove the spreading factor $r^{-\frac{1}{2}}$ from the acoustic pressure p and begin with the farfield wave equation

$$\frac{\partial^2 p}{\partial r^2} + \frac{\partial^2 p}{\partial z^2} - \frac{1}{\rho}\frac{\partial \rho}{\partial z}\frac{\partial p}{\partial z} = \frac{1}{c^2}\frac{\partial^2 p}{\partial t^2}, \tag{2.1}$$

where t is time, c is sound speed, and ρ is density. Equation (2.1) can be factored in two ways:

$$\frac{\partial p}{\partial r} = -\frac{1}{c_0}\sqrt{1 + \frac{\left(\frac{1}{c^2} - \frac{1}{c_0^2}\right)\frac{\partial^2}{\partial t^2} - \frac{\partial^2}{\partial z^2} + \frac{1}{\rho}\frac{\partial \rho}{\partial z}\frac{\partial}{\partial z}}{\frac{1}{c_0^2}\frac{\partial^2}{\partial t^2}}}\,\frac{\partial p}{\partial t} \tag{2.2}$$

$$\frac{\partial p}{\partial t} = -c_0\sqrt{1 + \frac{(c^2 - c_0^2)\frac{\partial^2}{\partial r^2} + c^2\frac{\partial^2}{\partial z^2} - c^2\frac{1}{\rho}\frac{\partial \rho}{\partial z}\frac{\partial}{\partial z}}{c_0^2\frac{\partial^2}{\partial r^2}}}\,\frac{\partial p}{\partial r}. \tag{2.3}$$

O The TDPE, which is the inverse Fourier transform of the PE, is obtained by approximating the square root in Eq. (2.2). The progressive wave equation (PWE) is derived from Eq. (2.3). The TDPE and PWE are valid to leading-order in domains in which range dependence is a perturbation.

A numerical solution of the PWE based on the method of alternating directions and nonlinear capability for the PWE have been developed, [14] and the PWE has been extended to handle density variations and sediment attenuation.[15] However, the PWE can not be extended to handle wide-angle propagation, and the TDPE is easier to initialize and is better suited to handle range-dependent problems.[16] Thus recent development has involved the TDPE, which has been extended to handle sediment dispersion and wide-angle propagation in shallow water.[16]

3. The higher-order TDPE

The 1-term Taylor series

$$\sqrt{1 + x} - 1 = \frac{1}{2}x + O(x^2) \tag{3.1}$$

Table I: Comparison of Taylor and Padé series.

x	4-term Taylor	1-term Padé	2-term Padé	3-term Padé	$\sqrt{1+x}$
0.25	1.11801	1.11765	1.11803	1.11803	1.11803
0.50	1.22412	1.22222	1.22472	1.22474	1.22474
0.75	1.31870	1.31579	1.32274	1.32287	1.32288
1.00	1.39844	1.40000	1.41379	1.41420	1.41421
1.25	1.45639	1.47619	1.49904	1.49996	1.50000
1.50	1.48193	1.54545	1.57931	1.58105	1.58114
1.75	1.46078	1.60870	1.65523	1.65812	1.65831
2.00	1.37500	1.72000	1.79584	1.80221	1.80278
2.50	0.91943	1.76923	1.86124	1.86994	1.87083
2.75	0.49545	1.81481	1.92376	1.93519	1.93649
3.00	-0.10156	1.85714	1.98361	1.99817	2.00000

has been used to derive the narrow-angle TDPE and the narrow-angle PWE, which are accurate for propagation angles up to about 15 degrees. The 1-term Padé series

$$\sqrt{1+x} - 1 = \frac{\frac{1}{2}x}{1+\frac{1}{4}x} + O(x^3) \tag{3.2}$$

has been used to derive a wide-angle TDPE for shallow water, which we refer to as TDPE$_s$ and which is accurate for propagation angles up to about 40 degrees. To obtain a higher-order TDPE that is accurate for the very wide propagation angles that occur near the source and over a hard ocean bottom, an approximation for the square root function that is very accurate for $x \cong 1$ is required. Since the Taylor series converges only for $|x| < 1$, many terms are required for $x \cong 1$.

The following generalization of Eq. (3.2) is not restricted to $|x| < 1$

$$\sqrt{1+x} - 1 = \sum_{j=1}^{n} \frac{a_{jn}x}{1+b_{j,n}x} + O(x^{2n+1}), \tag{3.3}$$

where n is the number of terms in the Padé series and

$$a_{j,n} = \frac{2}{2n+1} \sin^2 \frac{j\pi}{2n+1} \tag{3.4}$$

$$b_{j,n} = \cos^2 \frac{j\pi}{2n+1}. \tag{3.5}$$

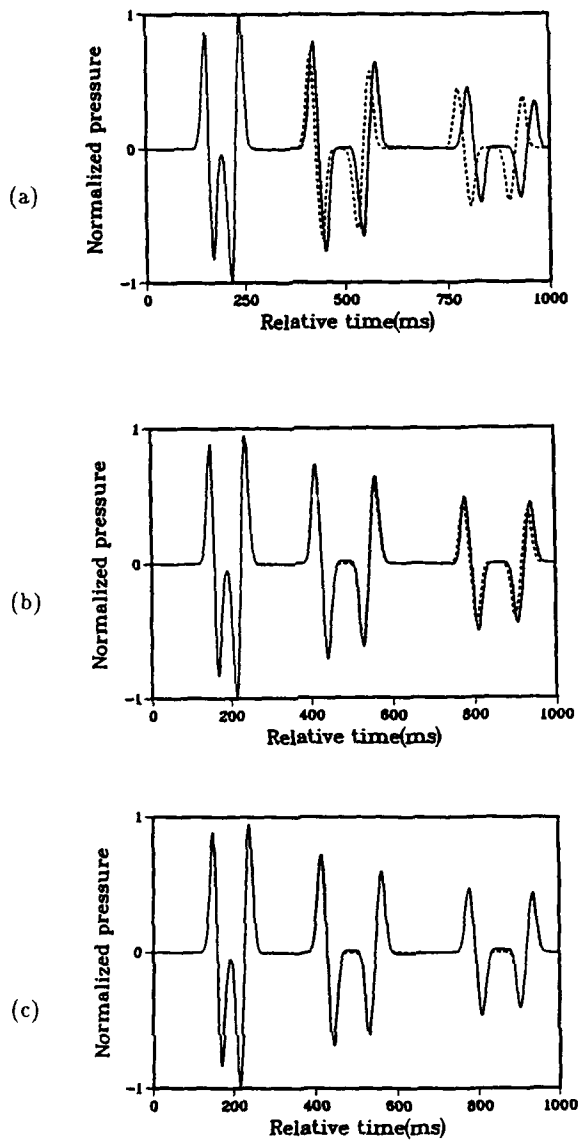

Figure 1: Time series at $r = 500$m and $z = 200$m for a Gaussian pulse in a waveguide with perfectly reflecting boundaries. The dashed curves are the image solution. The solid curves are the (a) TDPE_1, (b) TDPE_2, and (c) TDPE_3 solutions.

Since the Padé series is valid outside the radius of convergence of the Taylor series, relatively few terms are needed for $x \cong 1$. We illustrate this in Table I. The 4-term Taylor series is better than the 1-term Padé series for $x < 1$, but the 1-term Padé series is better for $x > 1$. The 2-term Padé series and the 4-term Taylor series are both correct to $O(x^5)$ for small x. Yet the 2-term Padé series is substantially better than the 4-term Taylor series. The 3-term Padé series is fairly accurate well beyond the radius of convergence of the Taylor series near $x = 3$.

The effects of attenuation and dispersion are less important than refraction and diffraction for most problems. Thus we do not derive corrections for the attenuation/dispersion operator in TDPE_s. For now, we assume that c is real (no attenuation) and independent of ω (no dispersion) in the analysis. From Eqs. (2.2) and (3.3), we obtain the following higher-order TDPE

$$\frac{\partial p}{\partial r} = -\left[\frac{1}{c_0} + \sum_{j=1}^{n} \frac{\alpha_{j,n}\frac{\partial^2}{\partial t^2} + \beta_{j,n}\left(\frac{\partial^2}{\partial z^2} - \frac{1}{\rho}\frac{\partial \rho}{\partial z}\frac{\partial}{\partial z}\right)}{\gamma_{j,n}\frac{\partial^2}{\partial t^2} + \delta_{j,n}\left(\frac{\partial^2}{\partial z^2} - \frac{1}{\rho}\frac{\partial \rho}{\partial z}\frac{\partial}{\partial z}\right)}\right]\frac{\partial p}{\partial t}, \tag{3.6}$$

where

$$\alpha_{j,n} = \frac{a_{j,n}}{c_0}\left(\frac{1}{c^2} - \frac{1}{c_0^2}\right) \tag{3.7}$$

$$\beta_{j,n} = \frac{-a_{j,n}}{c_0} \tag{3.8}$$

$$\gamma_{j,n} = \frac{1}{c_0^2} + b_{j,n}\left(\frac{1}{c^2} - \frac{1}{c_0^2}\right) \tag{3.9}$$

$$\delta_{j,n} = -b_{j,n}. \tag{3.10}$$

We define $u(r,z,t) = p(r,z,t + r/c_0)$ and rearrange Eq. (3.6) to obtain

$$\frac{\partial u}{\partial r} = -\left(\sum_{j=1}^{n}\frac{\alpha_{j,n}}{\gamma_{j,n}}\right)\frac{\partial u}{\partial t} - \sum_{j=1}^{n}\frac{\left(\beta_{j,n} - \frac{\alpha_{j,n}\delta_{j,n}}{\gamma_{j,n}}\right)\left(\frac{\partial^2}{\partial z^2} - \frac{1}{\rho}\frac{\partial \rho}{\partial z}\frac{\partial}{\partial z}\right)}{\gamma_{j,n}\frac{\partial^2}{\partial t^2} + \delta_{j,n}\left(\frac{\partial^2}{\partial z^2} - \frac{1}{\rho}\frac{\partial \rho}{\partial z}\frac{\partial}{\partial z}\right)}\frac{\partial u}{\partial t}. \tag{3.11}$$

We refer to Eq. (3.11) as TPDE_n. In the derivation of TDPE_s, it was assumed that

$$\left|\left(\frac{1}{c^2} - \frac{1}{c_0^2}\right)\frac{\partial^2 u}{\partial t^2}\right| << \left|\frac{\partial^2 u}{\partial z^2} - \frac{1}{\rho}\frac{\partial \rho}{\partial z}\frac{\partial u}{\partial z}\right|, \tag{3.12}$$

which is valid in shallow water. Since this assumption was not made to derive TDPE_n, we deduce that TDPE_1 is the generalization of the wide-angle PE to deep water.

4. Numerical solution

The alternating directions solution of TDPE_n requires numerical solutions for each of the following $n + 1$ equations

$$\frac{\partial u}{\partial r} + \left(\sum_{j=1}^{n} \frac{\alpha_{j,n}}{\gamma_{j,n}}\right)\frac{\partial u}{\partial t} = 0 \tag{4.1}$$

$$\gamma_{j,n}\frac{\partial^3 u}{\partial r \partial t} + \delta_{j,n}\left(\frac{\partial^2}{\partial z^2} - \frac{1}{\rho}\frac{\partial \rho}{\partial z}\frac{\partial}{\partial z}\right)\frac{\partial u}{\partial r} = -\left(\beta_{j,n} - \frac{\alpha_{j,n}\delta_{j,n}}{\gamma_{j,n}}\right)\left(\frac{\partial^2}{\partial z^2} - \frac{1}{\rho}\frac{\partial \rho}{\partial z}\frac{\partial}{\partial z}\right)\frac{\partial u}{\partial t}. \tag{4.2}$$

Since Eq. (4.1) is similar to the refraction term of TPDE_s, and Eq. (4.2) is similar to the diffraction term of TDPE_s, the numerical solution developed in Ref. 16 can be modified slightly to obtain the numerical solution of Eq. (3.11). Without the rearrangement of Eq. (3.6), it would be necessary to solve n equations similar to Eq. (4.2) as well as n third-order equations that are much more complicated than Eq. (4.1).

As in Ref. 16, the source function $f(t)$ is assumed to have compact support, and a time window $t_1 < t < t_2$ that contains the signal at all times is chosen. The boundary condition $u = 0$ is imposed at the pressure release surface, deep within the sediment at $z = z_M$ from which no energy returns to the water column due to attenuation, and after the signal has passed the obsever at $t = t_2$. The boundary conditions $u = \partial u/\partial t = 0$ are imposed before the signal is detected at $t = t_1$. Equation (4.1) is a first-order hyperbolic equation that can be solved with the Lax-Wendroff scheme[17].

Galerkin's method is used to discretize depth dependence in Eq. (4.2). The resulting equation is then solved with Crank-Nicolson integration in r using centered differences in t while sweeping from $t = t_1$ to $t = t_2$. We define the depth grid points $z_i = i\Delta z$. The basis functions $\Psi_i(z)$ vanish for $| z - z_i | > \Delta z$, increase linearly from 0 to 1 over $z_{i-1} < z < z_i$, and decrease from 1 to 0 over $z_i < z < z_{i+1}$. We define $u_i(r,t) = u(r, z_i, t)$ as well as $\Theta_i = \Theta(z_i)$ and $\Phi_i = \Phi(z_i)$ for arbitrary functions Θ and Φ. The basis functions provide the approximations

$$u(r,z,t) \cong \sum_i u_i(r,t)\Psi_i(z) \tag{4.3}$$

$$\Phi(z) \cong \sum_i \Phi_i\Psi_i(z) \tag{4.4}$$

$$\Theta(z) \cong \sum_i \Theta_i\Psi_i(z). \tag{4.5}$$

The depth operator Q_z is discretized with Galerkin's method, as follows:

$$Q_z\Phi|_{z=z_i} \cong \frac{\int \Psi_i Q_z \Phi dz}{\int \Psi_i dz}. \tag{4.6}$$

Substituting Eqs. (4.3), (4.4), and (4.5) into Eq. (4.6), we obtain the following approximations for the depth operators:

$$\Theta u\,|_{z=z_i} \cong \frac{\Theta_{i-1}+\Theta_i}{12}\,u_{i-1} + \frac{\Theta_{i-1}+6\Theta_i+\Theta_{i+1}}{12}\,u_i + \frac{\Theta_{i+1}+\Theta_i}{12}\,u_{i+1} \tag{4.7}$$

$$\Theta\frac{\partial^2 u}{\partial z^2}\,|_{z=z_i} \cong \frac{\Theta_i}{(\Delta z)^2}u_{i-1} - \frac{2\Theta_i}{(\Delta z)^2}u_i + \frac{\Theta_i}{(\Delta z)^2}u_{i+1} \tag{4.8}$$

$$\Phi\frac{\partial\Theta}{\partial z}\frac{\partial u}{\partial z}\,|_{z=z_i} \cong \frac{(\phi_{i-1}+2\Phi_i)(\Theta_{i-1}-\Theta_i)}{6(\Delta z)^2}\,u_{i-1} + \frac{\Phi_{i-1}(\Theta_i-\Theta_{i-1}) + 2\Phi_i(2\Theta_i-\Theta_{i-1}-\Theta_{i+1}) + \Phi_{i+1}(\Theta_i-\Theta_{i+1})}{6(\Delta z)^2}\,u_i + \frac{(\Phi_{i+1}+2\Phi_i)(\Theta_{i+1}-\Theta_i)}{6(\Delta z)^2}\,u_{i+1}. \tag{4.9}$$

5. Examples

To demonstrate the ability of TDPE_n to handle very-wide-angle propagation, we consider a waveguide of thickness 300m with pressure-release top and bottom boundaries in which c = 1500m/s. The Gaussian source $f(t) = \exp[-(\nu t)^2]$ is placed at z = 25m, where $\nu = 150\text{s}^{-1}$. The image solution, which is exact, is used to initialize the field at r = 200m, and we take c_0 = 1500m/s. The TDPE_1, TDPE_2, and TDPE_3 solutions are compared with the image solution in Figure 1.

Each of the solutions is very accurate for the first arrivals, which propagate at small angles. However, the agreement improves with n for the later arrivals, which propagate at larger angles.

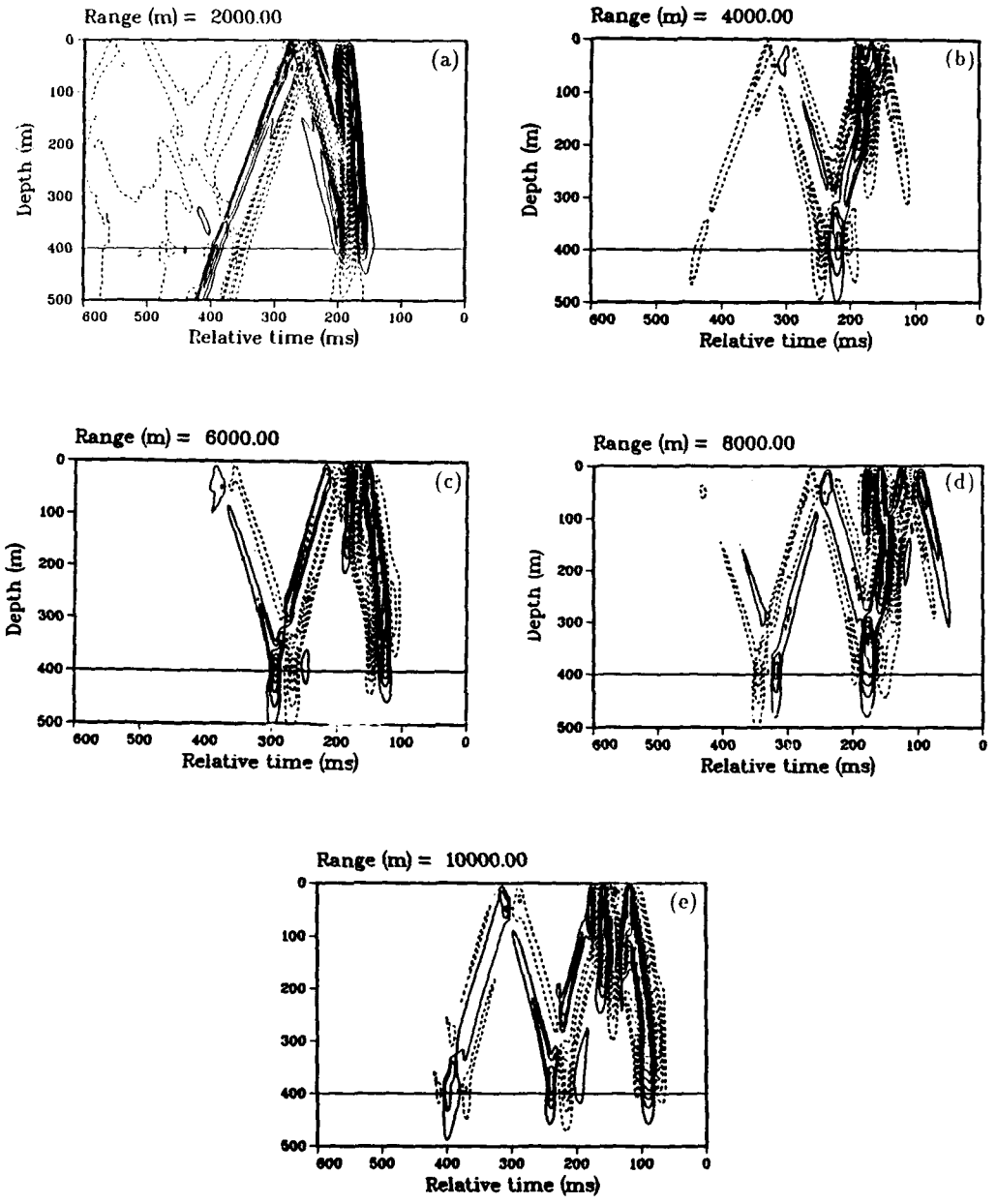

Figure 2: Contour plots of a Gaussian pulse in a refracting ocean.

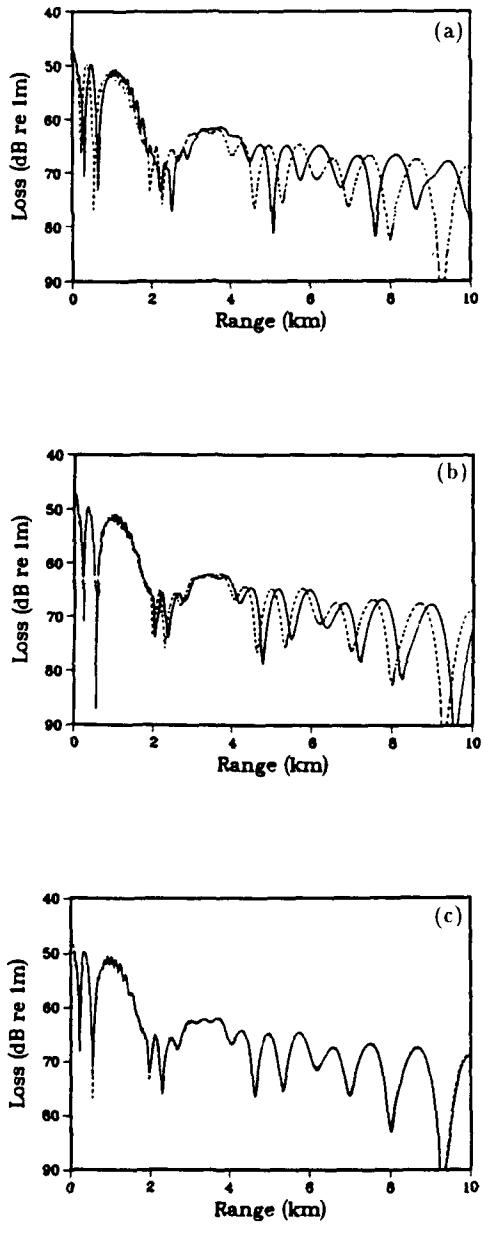

Figure 3: Transmission loss at $z = 390$m for a 50Hz source in a refracting ocean. The dashed curves are the wide-angle PE solution. The solid curves are the (a) narrow-angle PE, (b) TDPE_8, and (c) TDPE_1 solutions.

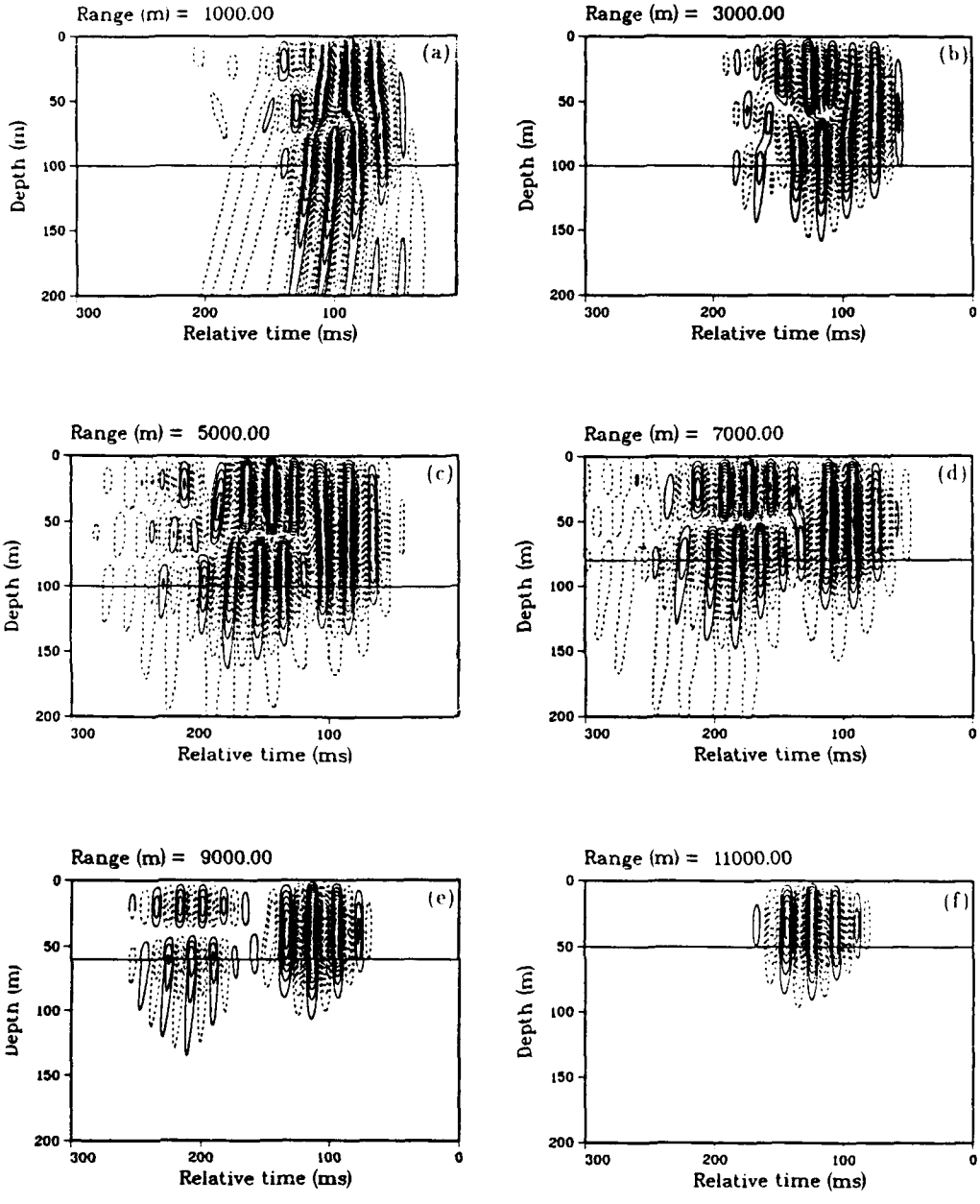

Figure 4: Contour plots of a Hanning weighted sinusoidal pulse in a range-dependent ocean.

In past studies of the TDPE, a stability condition for the numerical solution of the refraction operator has been discussed. However, the numerical solution of the diffraction operator appeared to be unconditionally stable based on numerical results. While performing the calculations for the previous example, however, we discovered a new stability condition involving the grid spacings Δz and Δt. In a homogeneous medium, the numerical solution of the diffraction operator is unstable for $\Delta z = c_0 \Delta t$ and $n > 1$. The solution appears to be stable for all n if $\Delta z > A c_0 \Delta t$, where numerical experiments give $A \cong 1.4$.

To demonstrate the ability of TDPE_n to handle large variations in sound speed, we consider an ocean of depth 400m in which c increases linearly from 1500m/s at $z = 0$ to 1600 m/s at $z = 400$ m (this is not intended to represent a realistic sound-speed profile). In the sediment, c = 1700m/s, $\rho = 1.5\text{g/cm}^3$, and the attenuation is $\beta = 0.5\text{dB}/\lambda$. The Gaussian source function with $\nu = 150\text{s}^{-1}$ is placed at $z = 50$m, and we take $c_0 = 1500$m/s. The homogeneous half-space field [18] is used as an initial condition at $r = 100$m. The plane-wave loss operator of Ref. 16 is used to model attenuation. However, we have found that greater accuracy is obtained by using c rather than c_0 in the loss operator. Sediment dispersion is neglected.

A sequence of contour plots of p computed with TDPE_1 appears in Figure 2. Solid contours correspond to $p > 0$; dashed contours correspond to $p < 0$. The solid line marks the ocean bottom. The response to f is convolved as in Ref. 16 to obtain the response to a 50Hz time-harmonic source. Transmission loss for the TDPE_1, TDPE_s, wide-angle PE, and narrow-angle PE solutions appears in Figure 3. The narrow-angle PE solution has large phase errors. The TDPE_s solution is better, but it too has a large error due to the strong refraction. The excellent agreement of the TDPE_1 and wide-angle PE solutions demonstrates the ability of TDPE_1 to accurately handle pulse propagation in deep water and shows that the plane-wave loss operator is accurate for this problem.

The phenomenon of mode cutoff in a range-dependent ocean has been illustrated for time-harmonic signals.[19] To illustrate energy cutoff in the time domain, we apply TDPE_1 in a range-dependent ocean in which the depth d is defined by

$$d(r) = \begin{cases} 100\text{m} & \text{for } r < 5\text{km} \\ \left(1 - \frac{r-5\text{km}}{10\text{km}}\right) 100\text{m} & \text{for } 5\text{km} < r < 10\text{km} \\ 50m & \text{for } r > 10km. \end{cases} \tag{5.1}$$

We take $c = 1500$m/s in the water and $c = 1600$m/s, $\rho = 1.5\text{g/cm}^3$, and $\beta = 0.5\text{dB}/\lambda$ in the sediment. The source function is the Hanning weighted sinusoid [20]

$$f(t) = \begin{cases} \left(1 - \cos \frac{1}{4}\omega t\right) \sin \omega t & 0 < t < T \\ 0 \text{ otherwise} \end{cases} \tag{5.2}$$

where $\omega = 100\pi s^{-1}$ and $T = 8\pi/\omega$. Since this source function has a fairly narrow frequency content, it is effective for illustrating normal mode behavior. The source is placed at $z = 25$m, and we apply the half-space field at $r = 100$m.

Snapshots of the TDPE_1 solution appear in Figure 4. The first three modes are clearly visible at $r = 5$km. The vertical dependence of the field matches the first mode for the first arrivals as only one extremum appears. A maximum and a minimum occur near $t = 150$ms due to arrivals of the second mode. The third mode, which has three extrema, is apparent for $t > 200$ms. Cutoff occurs for two of the modes as d decreases. The third mode is no longer evident at $r = 9$km. The second mode disappears by $r = 11$km.

6. Conclusion

A higher-order TDPE has been derived and solved numerically. Since the model is based on a Padé series that is very accurate and is not restricted to the unit circle in the complex plane, it is accurate for problems involving very wide-angle propagation as well as large sound-speed variations. Since the higher-order TDPE splits into terms similar to the refraction and diffraction terms of TDPE_s, it can be solved with similar methods. Although the coefficients of the terms in the higher-order TDPE are relatively complicated, they are easily handled with Galerkin's method. The higher-order TDPE solution is comparable in accuracy to outgoing coupled normal mode solutions. In particular, the model is valid in deep water.

Acknowledgments

This work was supported by the Office of Naval Research and the Naval Ocean Research and Development Activity.

References

[1] Tappert, F.D, "The Parabolic Approximation Method," in *Wave Propagation and Underwater Acoustics*, edited by J.B. Keller and J.S. Papadakis, Lecture Notes in Physics, Vol. 70, Springer, New York, 1977.

[2] Claerbout, J.F., *Fundamentals of Geophysical Data Processing*, McGraw-Hill, New York, 1976, 206-207.

[3] Botseas, G., Lee, D., and Gilbert, K.E., "IFD: Wide-Angle Capabilty," NUSC Tech. Rep. 6905, 1983.

[4] Greene, R.R., "The Rational Approximation to the Acoustic Wave Equation with Bottom Interaction," *J. Acoust. Soc. Am.*, 1984, 76, 1764-1773.

[5] McDaniel, S.T. and Lee, D., "A Finite-Difference Treatment of Interface Conditions for the Parabolic Equation: The Horizontal Interface," *J. Acoust. Soc. Am.*, 1982, 71, 855-858.

[6] NORDA Parabolic Equation Workshop," edited by J.A. Davis, D. White, and R.C. Cavanagh, NORDA Tech. Note 143, 1982.

[7] Bamberger, A., Engquist, B., Halpern, L., and Joly, P., "Higher Order Paraxial Wave Equation Approximations in Heterogeneous Media," *SIAM J. Appl. Math.*, 1988, 48, 129-154.

[8] Collins, M.D., "Benchmark Calculations for Higher-Order Parabolic Equations," *J. Acoust. Soc.*

Am., to appear.

[9] Evans, R.B., "A Coupled Mode Solution for Acoustic Propagation in a Waveguide with Stepwise Depth Variations of a Penetrable Bottom," *J. Acoust. Soc. Am.*, 1983, 74, 188-195.

[10] Nghiem-Phu, L. and Tappert, F.D., "Modeling of Reciprocity in the Time Domain Using the Parabolic Equation Method," *J. Acoust. Soc. Am.*, 1985, 78, 164-171.

[11] Jensen, F.B., "Wave Theory Modeling: A Convenient Approach to CW and Pulse Propagation Modeling in Low-Frequency Acoustics, *IEEE J. Ocean. Eng.*, 1988, 13(4), 186-197.

[12] Claerbout, J.F., *Fundamentals of Geophysical Data Processing*, McGraw-Hill, New York, 1976, 208-215.

[13] Murphy, J.E., "Finite-Difference Treatment of a Time-Domain Parabolic Equation: Theory," *J. Acoust. Soc. Am.*, 1985, 77, 1958-1960.

[14] McDonald, B.E. and Kuperman, W.A., "Time Domain Formulation for Pulse Propagation Including Nonlinear Behavior at a Caustic," *J. Acoust. Soc. Am.*, 1987, 81, 1406-1417.

[15] Collins, M.D., "Low-Frequency, Bottom-Interacting Pulse Propagation in Range-Dependent Oceans," *IEEE J. Ocean. Eng.*, 1988, 13(4), 222-228.

[16] Collins, M.D., "The Time-Domain Solution of the Wide-Angle Parabolic Equation Including the Effects of Sediment Dispersion," *J. Acoust. Soc. Am.*, 1988, 84, 2114-2125.

[17] Mitchell, A.R. and Griffiths, D.F., *The Finite Difference Method in Partial Differential Equations*, Wiley, New York, 1980, 59-70.

[18] Collins, M.D., "A Nearfield Asymptotic Analysis for Underwater Acoustics," *J. Acoust. Soc. Am.*, 1989, 85, 1107-1114.

[19] Jensen, F.B. and Kuperman, W.A., "Sound Propagation in a Wedge-Shaped Ocean with a Penetrable Bottom," *J. Acoust. Soc. Am.*, 1980, 67, 1654-1566.

[20] Schmidt, H., "SAFARI User's Guide," SACLANT Undersea Research Centre, La Spetzia, Italy, 1988.